Nanostructured, Functional Films Prepared Using Thermionic Vacuum Arc

C.P. LUNGU[1], I. JEPU[1], I. MUSTATA[1], V. KUNCSER[2], V. IONESCU[3],
V. CIUPINA[3], M. OSIAC[4], G.E. IACOBESCU[4]

[1]INCD pentru Fizica Laserilor, Plasmei si Radiatiei
E-mail: cristian.lungu@inflpr.ro
[2]INCD pentru Fizica Materialelor
[3]"Ovidius" University, Constanta
[4]Faculty of Physics, Craiova University

1. Introduction

Nanostructured magnetoresistive systems based on ferromagnetic materials have been the subject of intensive study due to their relevance both in fundamental physics and in technological applications connected with digital data storage and spintronics, such as reading heads and sensors, high density media, magnetic random access memories. Transport properties in granular structures where ferromagnetic grains are separated by non magnetic spacers are affected by spin-dependent electron confinement and spin filtering, leading to oscillating magnetic coupling and tunneling magnetoresistance.

The structure degree of resistance is extremely variable in the presence of the magnetic field in comparison with the resistance in its absence. The magnetic grains have a super paramagnetic behavior, easily to be oriented to an exterior magnetic field. In its absence, they return to the disordered orientation of the spins they had before the magnetic field application.

The tunneling barrier height depends on the insulator nature; this is why we prepared MgO matrix and the respective MgF_2 matrix magnetoresistive films for a comparative study of the magnetoresistance behavior with the two isolators.

Taking into consideration that the MgF_2 coatings have special optical properties, the so called anti-reflection coatings were prepared with this substance, and we have measured optical absorption of the coated layers in 200-1000 nm domain.

2. Deposition Method

The magnetic metal concentration in the insulator matrix plays a very important role in reaching a tunneling magnetoresistance effect. A mixture of MgF_2 and cobalt was prepared to observe the factors' influence. In order to observe the concentration influence on the magnetoresistance effect, MgF_2 and Co were simultaneously evaporated on 0.5 mm thickness microscope glass slides set above two thermionic vacuum arc evaporation sources as presented in Fig. 1 and more detailed in ref. [2], to both benefit from the coating speed variation and the distance of the evaporation source place.

After that, we heated the MgF_2 and Co anodes keeping the electrical parameters at constant values (the intensity of the filament current, the intensity of the discharge current, and the applied voltage) and the shutter close.

After the electrical parameters remained constant, the shutter screen was removed until the desired thickness was reached. In this case we used the following formula in order to calculate the average density of the prepared compound, the value that must be introduced as parameter of the thickness measurement unit. Let's suppose we intend to prepare a compound with the ratio of the atom concentrations to be **a/b**. We take as reference a volume of 1 cm^3. We suppose that the volume of the material A is V_A and the volume of the material **B** is V_B. We have:

$$V_A + V_B = 1 \tag{1}$$

The masses of the two materials are $\rho_A V_A$ and $\rho_B V_B$ respectively, where ρ is the material density. The number of the atoms of each material will be:

$$n_A = [\rho_A V_A/\mu_A]*N \quad \text{and respectively} \quad n_B = [\rho_B V_B/\mu_B]*N \tag{2}$$

where N is the Avogadro's number and μ is the respective molar mass.
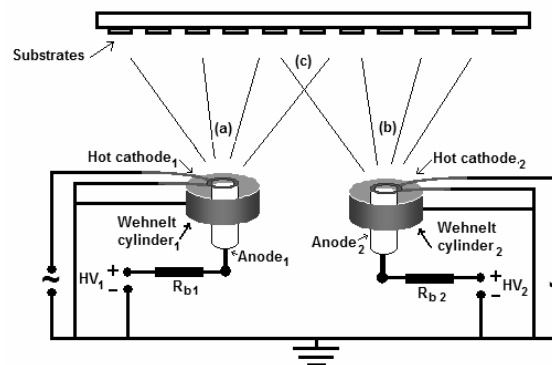

Fig. 1. Experimental set-up. a) Plasma produced in MgF_2 vapors, b) plasma produced in Co vapors, c) zone of mixed plasmas.

Finally we obtain:

$$n_A/n_B = [\rho_A V_A/\mu_A] / [\rho_B V_B/\mu_B] = a/b \qquad (3)$$

Using eq. (3) and eq. (1) we obtain V_A and V_B which are introduced into the following equation:

$$\rho_A V_A + \rho_B V_B = \rho_{med}(V_A + V_B) \qquad (4)$$

When two materials are co-deposited the compound density is calculated and settled on the measuring unit.

3. Results and Discussion

The coated films were analyzed by transmission electron microscopy (TEM) using a PHYLIPS CM 120 apparatus at Ovidius University, Constanta where was inferred the nano-metrical structure of the Co magnetic particles uniformly spread in the dielectric matrix of MgF_2. (Fig. 2).

Using TEM, it was observed the nanosize dimension of the magnetic grains (2-3 nm), which leads to the over paramagnetic structure of those domains, very useful in reaching uniform domains through post deposition thermal treatment [3-7]. The selected area diffraction pattern, presented in Fig. 3 shows diffuse rings due to the Co grains embedded in the MgF_2 matrix, as well as specific patterns due to the formation of the crystalline Co grains.
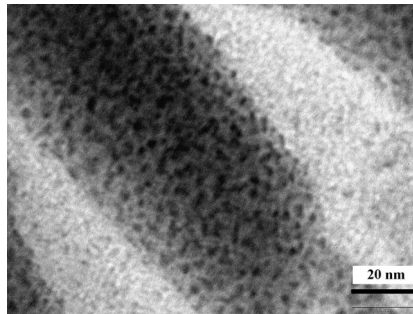

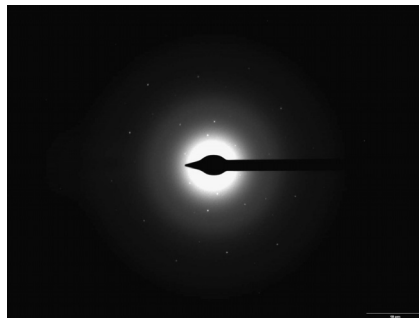**Fig. 2.** TEM image of the MgF_2-40at%Co film.

Fig. 3. Selected area diffraction of the $MgF_2$40%atCo film.
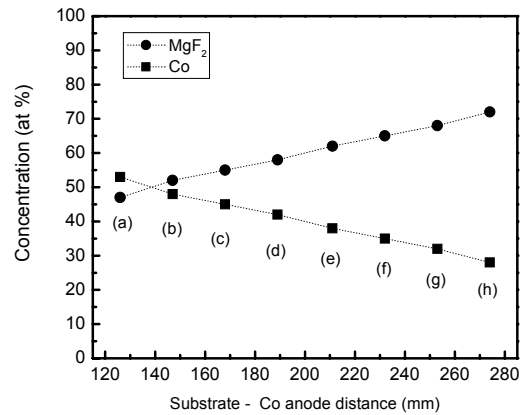
Fig. 4. Co and MgF$_2$ concentration in the studied samples,
measured by energy dispersive spectroscopy (EDS).

The relative amount of Co (at. %), as obtained by EDS measurements on different samples, versus the distance from the Co crucible to the film supports, is presented in Fig. 4 (e.g. sample (a) corresponds to a distance of 125 mm, whereas the sample (h) is the sample placed at a distance: Co anode - substrate of 275 mm). The distance between the two anodes was 150 mm. It was observed the almost linear decrease of the Co concentration with the increasing distance between the substrate and the Co anode.

As a consequence of the different Co contents in the different samples from the sample (a), to the sample (h), it was studied the dependence of the TMR effect and the related structural and magnetic behaviors versus the concentration of the magnetic element. It is worth mentioning that the thickness of the central samples (d) and (e) was 250 nm and the other samples present thicknesses of the same magnitude inside the measuring error bars.
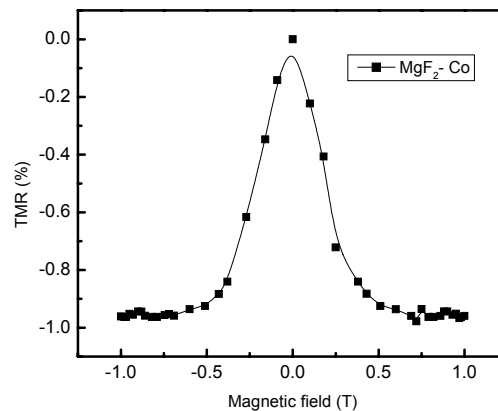

Fig. 5. Tunneling magnetoresistive response of the MgF$_2$40%Co
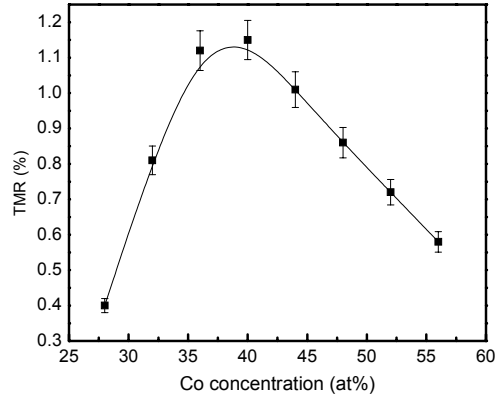sample film versus the applied magnetic field.

Fig. 6. The room temperature TMR effect for different
concentrations of Co in the MgF_2 matrix.

The variation of the TMR effect at room temperature (RT) defined as the $(R_H-R_0)/R_0$ was measured in a current in plane (CIP) arrangement. Fig 5 shows the magnetoresistive response of the MgF_2 40 % Co sample film versus the applied magnetic field, while the TMR response versus the relative content of cobalt in the magnesium fluoride dielectric film is shown in Fig. 6.

It is easily observed that the TMR effect has a maximum value at a given Co concentration (40 at % Co in this case) and decreases much faster at lower Co concentration as compared with the case of higher Co concentrations in the range of 40 to 57 at % Co. Most likely, this effect has to be related with different morphology or size distribution of the Co particles in the dielectric matrix and we will return to this point after providing structural and magnetic data.

Fig. 7 shows the longitudinal magneto-optic Kerr effect (MOKE) hysterezis loop obtained at RT on MgF_2 40 % Co sample.
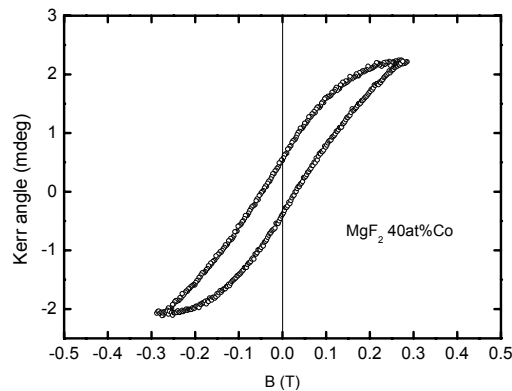

Fig. 7. The magneo-optic Kerr effect behavior of the MgF_2 40 % Co
sample versus the magnetic field.

In order to correlate TMR effect and magnetic data, we will further show some structural and magnetic aspects of the film containing MgF_2 40 % Co. Both the as prepared sample, as well as the annealed one were analyzed and processed by a post-deposition thermal treatment, performed at 300^0C for one hour in high vacuum condition (10^{-5} torr).

The EDS spectra collected on the two samples have shown slightly increased oxygen content in the annealed sample as compared with the as-prepared one, which would lead presumably to an increased partial oxidation of the Co particles in the annealed sample. The scanning electron microscopy (SEM) images of the as-deposited and the annealed MgF_2 40 % Co film, presented in Fig. 8 and Fig. 9 respectively, show clearly much larger grains induced by the thermal treatment. Electron diffraction patterns evidence that the structure with well arranged atomic planes belongs to metallic Co grains, of which dimensions are much larger in the thermally annealed sample as compared with the as-prepared one.
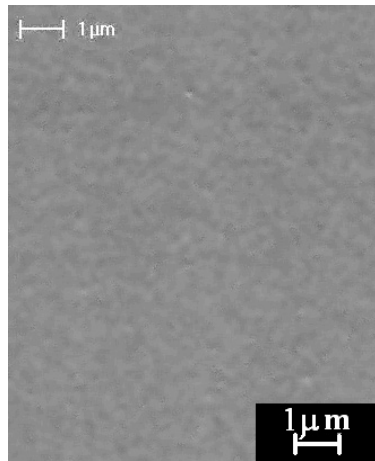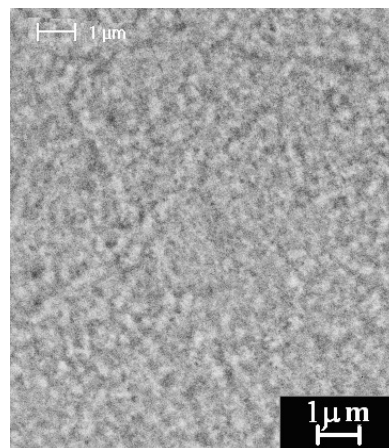

Fig. 8. SEM image of the as-deposited MgF_2 40 % Co sample.

Fig. 9. SEM image of the annealed MgF_2 40 % Co sample.

In addition, the electron diffraction has proven the presence of cobalt oxide (the antiferromagnetic Co_3O_4) in both the as-prepared sample and the annealed sample. The amount of the cobalt oxide is slightly larger in the annealed sample, in agreement with the EDS data proving increased oxygen content in this sample.

The RT MOKE hysteresis loops of the as-prepared and annealed MgF_2 40 % Co films are presented in Fig. 10. One can see that the thermal treatment increases the saturation magnetization of the film as well as its coercive force. Based on this structural/morphologic picture of the two samples, we can interpret the corresponding RT MOKE curves as follows. In the as-prepared sample, there are formed very fine Co grains (about 5 nm) with a thin magnetic dead layer of cobalt oxide, giving rise to a reduced magnetization of the sample (due to both defected spin structure and possible superparamagnetic behavior of the grains of lower dimensions).
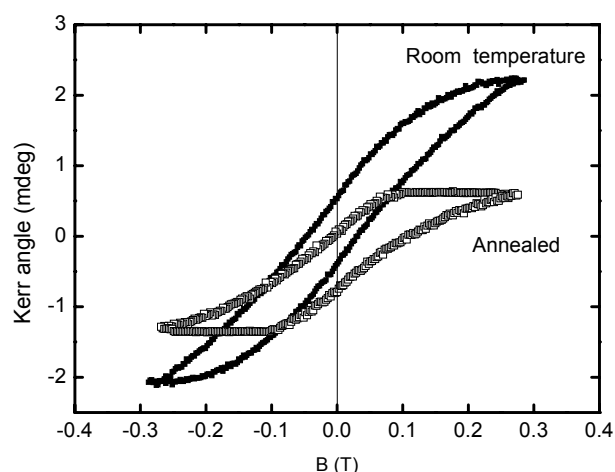

Fig. 10. Room temperature MOKE measurements of the as-prepared and the annealed at $300^{O}C$ MgF_2 40 % Co film.

After the annealing treatment, the initial clusters agglomerate giving rise to much larger Co crystalline particles. In spite of a slightly thicker cobalt oxide layer on the surface, the Co core is significantly larger than in the case of the as-prepared film, which leads finally to higher average magnetic moment per Co atom, due to both a less defected magnetic structure and reduced magnetic relaxation of the Co particles. Hence, a higher magnetization and coercive field is expected for the annealed sample.

The magnetic field dependent TMR response of the annealed samples showed a decrease of the magnetoresistance in comparison with the as-prepared ones. That is probably due to increased distances between the magnetic grains in the annealed samples (directly connected with formation of much larger magnetic grains), diminishing drastically the tunneling probability in this system. Hence, the thermal

treatment appears to decrease the TMR coefficient in MgF_2 - Co systems, opposite to the effect of similar treatments applied to nanoglobular GMR systems like Co-Cu or Fe-Cu [8].

The above observation can be also extended to the case of the TMR data presented in Fig. 6. The continuous decrease of the magnetization with the Co relative content in the films has to be explained by a reduced average size of the Co grains (and implicitly by an increased particle density) in films of higher Co content. That would explain the fast increase of the TMR effect when increasing the Co content in the film up to the optimal value of 40 at. %. However, by further increasing the Co content, the TMR effect starts to decrease, due to an enhanced magnetic disorder specific to the very large surface area of very fine particles, connected also with a very weak magnetic response to the applied field.

The transmission coefficient decreases in the intervals of 328 nm - 498 nm, Zone I and 500 nm-900 nm, Zone II, respectivelly, with the increase of the Co concentration into the MgF_2 matrix. The maximum peaks of transmission move also from 394 to 370 nm, Zone I, and from 700 nm to 570 nm in Zone II for the films with higher concentration of Co (from 26 a t% Co to 56 at % Co).

Between 970 and 1200 nm, the transmission coefficients of the all films are almost the same, with very high (0.98 to 0.99), with a tendency for the films with higher concentration in Co to be higher than the others.
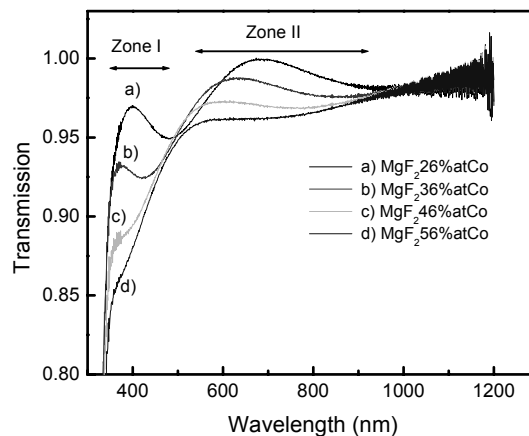

Fig. 11. Transmission spectra of MgF_2-Co films.

This behavior of the transmission could be due to the refraction indices of the films with different concentration of Co magnetic clusters. We expect also the diffraction of the light due to the nanometric grain size of Co clusters embedded into the MgF_2 matrix.

The dependence of the transmission on Co cluster concentration in Zone I and Zone II could be explained as in ref [11] on the trasmission decrease as function of film thickness, in our case the increasing of the Co grain concentration. The

minimum of the transmission will be correlated with the "percolation threshold" - the situation when the Co clusters form a continuum film. The reason why that happens is because the electrons are trapped in individual islands and cannot move freely like in a closed film. The electromagnetic field of an incoming lightwave can excite surface plasmons which lead to absorption [12].

The films could be used as absorption filter on different range of the wavelength, controlled by the magnetic nanometric size and the cluster concentration.

4. Conclusions

MgF_2-Co granular films presenting TMR effects were successfully prepared by the TVA method. The films with different Co cluster concentrations were obtained by settling film substrates at different distances from the Co and MgF_2 evaporation sources. A maximum TMR effect of about 1.2 % was obtained at room temperature for a relative content of 40 at % Co. High resolution TEM and electron diffraction measurements reveal the presence of the crystalline Co grains as well as surrounding shells of cobalt oxide. Post deposition thermal treatments of the Co-MgF_2 films (for one hour, $300^{o}C$, 10^{-5} torr) increase substantially the average of the Co grain size and slightly the thickness of the cobalt oxide layers around nanograins. These structural results support the increased magnetization in the room temperature MOKE hysterezis loop in the annealed samples as well as the decreased TMR effect, due to increasing distances among Co nanograins.

The proposed processing method (TVA) allows the fast deposition of TMR granular structures with a large variation of the concentration of the magnetic metal in the insulating matrix. However, the TMR effects in such systems are still low and further work is needed in order to improve them.

References

[1]   BADER S.D., ERSKINE J.L., in: B. Heinrich, J.A.C., Bland (Eds.), Ultrathin Magnetic Structures, Springer Verlag, Berlin, 1994.
[2]   MUSTATA I., *et al*., Vacuum, ,**76,** p. 131., 2004.
[3]   MOODERA J.S. and MESERVEY R.H., 2004 *Magnetoelectronics* Ed M.Johnson, (Academic Press).
[4]   JULLIERE M., *Phys. Lett.,* **54 A** 225, 1975.
[5]   TSYMBAL E.Y., MRYASOV O.N., LECLAIR P.R., *J. Phys.: Condens. Matter*, **15,** 109, 2003.
[6]   KUNCSER V., *et al.*, *Surf.& Coat. Techn*, **1-4**, 980, 2005.
[7]   LUNGU C.P., *et al.*, *Surf and Coat. Techn*, **200**, 399, 2005.
[8]   ANGHEL A., *et al.*, *Czech J. Phys.*, **56 B,** 16, 2006.
[9]   KUNCSER V., *et al.*, Journal of Alloys and Compounds, **499,** 23, 2010.
[10]   IONESCU V., *et al.*, *Thin Solid Films*, **518,** 3945, 2010.
[11]   CHARTON C. and FAHLAND M., *Surf.and Coat. Techn.*, **174-175**, 181, 2003.
[12]   ABELÈS F., BORENSZTEIN Y., LÓPEZ-RIOS T., Festkörpeprprobleme XXIV (1984).